Resonance energy transfer in arbitrary media: Beyond the point dipole approximation

K. Nasiri Avanaki,[1] Wendu Ding,[1] and George C. Schatz[1,*]

[1] *Department of Chemistry, Northwestern University,*

2145 Sheridan Road, Evanston IL 60208-3113, United States

In this work, we present a comprehensive theoretical and computational study of donor/acceptor resonance energy transfer (RET) beyond the dipole approximation, and including for arbitrary inhomogeneous and dispersive media. The theoretical method extends Förster theory for resonance energy transfer between donor and acceptor molecules or nanoparticles to the case where higher multipole transitions in the donor and acceptor play a significant role in the energy transfer process. In our new formulation, the energy transfer matrix element is determined by a fully quantum electrodynamic expression, but its evaluation only requires classical electrodynamics calculations. By means of a time-domain electrodynamical approach (TED), the matrix element evaluation involves the electric and magnetic fields generated by the donor and evaluated at the position of acceptor, including fields associated with electric dipoles, electric quadrupoles and magnetic dipoles in the donor, and the acceptor response to the electric and magnetic fields and to the electric field gradient. As an illustration of the benefits of the new formalism, we tested our method with a 512-atom lead sulfide (PbS) quantum dot as donor/acceptor either in vacuum or with a spherical nanoparticle(toy model) in the surrounding medium. This includes an analysis of the effects of interferences between multipoles in the energy transfer rate. The results show important deviations from the conventional Förster dipole theory that are important even in vacuum, but which can be amplified by interaction with a plasmonic nanoparticle.

* g-schatz@northwestern.edu

I. INTRODUCTION

Förster resonance energy transfer (FRET), resulting from donor/acceptor dipole-dipole interactions was originally developed in 1948 [1], and it was used for the first time in 1967 as a spectroscopic ruler to measure distances in macromolecules[2]. Such optical rulers based on FRET opened a new era for a wide range of biological studies where nonzero spectral overlap between donor emission and acceptor absorption plays a key role. As is discussed in several articles [3, 4], the distance dependent criteria restricts the length scale of FRET rulers to a maximum of about 10 nm, which means that normal FRET optical rulers are not suitable for the investigation of many biological structural changes that take place at longer length scales [5].

This type of energy transfer from a donor species initially in an excited electronic state to an acceptor in its ground state, possesses features that have been under a great deal of attention, both theoretically and experimentally, particularly in nanoscience and technology. Moreover, the science of resonance energy transfer has been broadly explored in artificial light harvesting antenna devices [6, 7], spasers [8, 9], and especially in biology as an assessment method for studying the dynamical evolution of energy [10]. The study of these phenomena in nanostructures has recently led to promising applications in solar cell systems [11, 12] and optical switching [13, 14].

Semiconductor quantum dots (QDs) have sometimes been used as novel light harvesters in solar cells, where FRET induced by electronic coupling between QDs plays an essential role in the function of such devices. However, FRET, based on the point dipole approximation, is only valid if the donor-acceptor distance is significantly larger than the size of the donor or acceptor. For closely placed donor-acceptor systems, various adjustments to the FRET approximation have been suggested, like atom-centered transition charges [15], continuous transition densities [16], or partial dipoles [17].

Past studies of FRET in QD films have emphasized the key role of higher order multipole interactions in exciton transfer between closely packed QDs [18]. When the donor-acceptor distance is beyond the van der Waals effective regime, and Coulombic interaction between the transition densities of the chromophores [19] is their primarily coupling, as long as the emission and absorption transitions are electronically allowed, the type of interaction occurring between transition dipoles is known as the "ideal dipole approximation" (IDA)

[20–22]. Here the Coulombic interaction between donor and acceptor defines the rate of energy transfer between these two. IDA is an excellent approximation for energy transfer at visible photon energies, since the wavelength of light in this case is much larger (several hundred times) than the size of the molecule. In other words, the coupling matrix element is not sensitive to any variation in the vector potential which may be present over the spatial extent of the transition densities of the donor or acceptor. However an asymmetric shape to the transition densities and/or large spatial extent may make the IDA invalid. This is also an issue when the transition is dipole forbidden or only weakly allowed. Under these circumstances, the transition dipole moment is not sufficient to represent the the spatial distribution of the transition density, and the IDA is not applicable. A more accurate description of the Coulombic interaction between transition densities would involve the use of more terms from the multipolar expansion for donor emission and/or acceptor absorption. In addition, since the electromagnetic field due to the donor may be highly nonuniform over the extent of the acceptor, it may be important to couple field gradients to the multipole expansion in determining energy transfer rates. This is especially important for emitters and absorbers that are nanoparticles of sufficient size, as size can easily activate higher multipole forbidden transitions.

Recently, Ding et al.[23, 24] have presented a general computational scheme to simulate RET in inhomogeneous absorbing and dispersive media using a real-time electrodynamics approach; the time-domain electrodynamics resonance energy transfer (TED-RET) method. Applications of this method have considered plasmon-coupled resonance energy transfer in which there is a plasmonic particle in the medium near to the donor and acceptor, and this leads to substantial enhancements in both the rate and range associated with energy transfer. In their approach the donor is assumed to be a single radiating molecule positioned at r_D whose size is much smaller than the distance between the donor and the acceptor. In this case, it is appropriate to make the point-dipole approximation, $\mathbf{P}_{ex}(\mathbf{r},t) = \mathbf{p}_{ex}(t)\delta(\mathbf{r}-\mathbf{r}_D)$, in which the external polarization $\mathbf{P}_{ex}$ generated by the donor in a dielectric medium is defined by $\mathbf{p}_{ex}(t)$. In the TED-RET approach, the transition matrix element, at angular frequency ω, is calculated from the electric field $\mathbf{E}^D(\mathbf{r}_A)$ at the position of the acceptor ($\mathbf{r}_A$) originating from the donor at position $\mathbf{r}_D$ using the following expression:

$$M^{ee}(\mathbf{r}_D,\mathbf{r}_A,\omega) = -\mu^{eg}(\mathbf{r}_A)\mu^{ge}(\mathbf{r}_D)\frac{\mathbf{e}_A.\mathbf{E}^D(\mathbf{r}_A,\omega)}{p_{ex}(\omega)} \tag{1}$$

Here $\mu^{eg}(\mathbf{r}_A)(\mu^{ge}(\mathbf{r}_D))$ represents the magnitude of the transition dipole of the donor (acceptor) and the superscript $e(g)$ stands for the excited(ground) states, while the orientation of acceptor transition dipole is defined by the unit vector $\mathbf{e}_A$. Employing Fermi's Golden rule, the rate of energy transfer is expressed as

$$W_{D\longrightarrow A} = \frac{2\pi}{\hbar}|M^{ee}(\mathbf{r}_A, \mathbf{r}_D, \omega)|^2 \rho(\omega) \tag{2}$$

where $\rho(\omega)$ is the density of final states associated with energy $\hbar\omega$ (corresponding to the exciton energy). This formulation has several advantages: (i) electric and magnetic fields can be obtained from standard computational electromagnetic software, such as the finite difference time domain method (FDTD) or Mie theory; (ii) transition dipoles for both the donor and the acceptor can be calculated via quantum chemistry software such as time-dependent density functional theory(TD-DFT); and (iii) it is valid for any inhomogeneous, absorbing, and dispersive media. Indeed, evalution of the field $\mathbf{E}^D$ in the time domain is often desirable for such media, which is why the theory is referred to as the TED-RET approach.

However, when the optical transition in the donor and/or acceptor is dipole forbidden, or the size of the donor and/or the acceptor is comparable with distance between them, the dipole approximation is not valid any more and the effect of higher order multipoles needs to be included. Here, we present a general but simple computational scheme, to mimic RET in inhomogeneous, absorbing, and dispersive media, but going beyond the dipole approximation to include magnetic dipole and electric quadrupole effects. As part of this approach, we show that the transition matrix elements for RET ($M(\mathbf{r}_D, \mathbf{r}_A, \omega)$) can be expressed in terms of interactions between acceptor transition multipoles (electric dipole, magnetic dipole, and electric quadrupole) and the corresponding electromagnetic fields generated by the donor transition multipoles.

II. ELECTRODYNAMICS OF MULTIPOLE FIELDS

The electromagnetic fields generated by electric and magnetic dipoles at the observation point $\mathbf{r}$ produced by current densities $\mathbf{J}(\mathbf{r}', \omega)$ in the infinitesimal volume $d^3\mathbf{r}'$ located at $\mathbf{r}'$ in the space-frequency domain are [25]

$$\begin{aligned}\mathbf{E}(\mathbf{r};\omega) &= i\mu_0\omega \int_{-\infty}^{\infty} d^3r' \overleftrightarrow{G}(\mathbf{R};\omega).\mathbf{J}(\mathbf{r}',\omega) \\ \mathbf{B}(\mathbf{r};\omega) &= \frac{i\mu_0\omega}{c} \int_{-\infty}^{\infty} d^3r' \overleftrightarrow{G}^m(\mathbf{R};\omega).\mathbf{J}(\mathbf{r}',\omega)\end{aligned} \tag{3}$$

where $\mathbf{R} = \mathbf{r} - \mathbf{r}'$.

The standard Green's functions $\overleftrightarrow{G}$ and $\overleftrightarrow{G}^m$, relate the electric and magnetic fields to the particle current density and can be expressed in a variety of different forms, which are physically equivalent. It is of interest to express the Green's functions for the electric and magnetic fields in spherical coordinates centered on $\mathbf{R} = 0$. Closed-form expressions are obtained for the Green's function of the electric field, $\overleftrightarrow{G}(\mathbf{R};\omega)$, and the Green's function of the magnetic field, $\overleftrightarrow{G}^m(\mathbf{R};\omega)$ in these coordinates in vacuum [25] as

$$\begin{aligned}\overleftrightarrow{G}_{vac}(\mathbf{R};\omega) &= \frac{ik}{4\pi}\left[\frac{1}{ikR}\left(\overleftrightarrow{U} - \hat{\mathbf{R}}\hat{\mathbf{R}}\right) - \left[\frac{1}{(ikR)^2} - \frac{1}{(ikR)^3}\right]\left(\overleftrightarrow{U} - 3\hat{\mathbf{R}}\hat{\mathbf{R}}\right)\right] e^{i\mathbf{k}.\mathbf{R}}, \\ \overleftrightarrow{G}^m_{vac}(\mathbf{R};\omega) &= \frac{ik}{4\pi}\left[\frac{1}{ikR} - \frac{1}{(ikR)^2}\right] e^{i\mathbf{k}.\mathbf{R}} \overleftrightarrow{U} \times \hat{\mathbf{R}},\end{aligned} \tag{4}$$

where $\mathbf{k}$ is the wavevector, $k = \omega/c$ is the wave number, $R = |\mathbf{R}|$ is the distance from the source to the observation point, and $\overleftrightarrow{U} = \hat{\mathbf{R}}\hat{\mathbf{R}} + \hat{\boldsymbol{\Theta}}\hat{\boldsymbol{\Theta}} + \hat{\boldsymbol{\Phi}}\hat{\boldsymbol{\Phi}}$. A more general form of the Green's function is discussed in the Supporting Information (SI). Assuming the permeability of the achiral media is close to 1 ($\mu = \mu_0$ which is true for water, silver, and copper), in the absorbing and dispersive, but still homogeneous, media [26]

$$\begin{aligned}\overleftrightarrow{G} &= \epsilon_r^{-1}\left[(\epsilon_r + 2)/3\right]^2 \overleftrightarrow{G}_{vac}(n(\mathbf{r},\omega)\mathbf{k}) \\ \overleftrightarrow{G}^m &= \epsilon_r^{-1}\left[(\epsilon_r + 2)/3\right]^2 \overleftrightarrow{G}^m_{vac}(n(\mathbf{r},\omega)\mathbf{k})\end{aligned} \tag{5}$$

Now, if the source current density distribution is narrowed down to a spatial region ($\delta(\mathbf{r})$ where $\mathbf{r}$ is the spatial position of the source) much smaller than the typical wavelength of the corresponding field, then the emitted field can be calculated on the basis of a multipole expansion of the current density in k-space as:[25]

$$\mathbf{J}(\mathbf{k};t) = \sum_{n=0}^{n=\infty} \frac{1}{n!}(\mathbf{k}\cdot\nabla_k)^n \mathbf{J}(\mathbf{k}=\mathbf{0};t) \tag{6}$$

where,

$$\mathbf{J}(\mathbf{k}=\mathbf{0};t) = \int_{-\infty}^{+\infty} \mathbf{J}(\mathbf{r},t)d^3\mathbf{r} \equiv \mathbf{J}^{ED}(t) \tag{7}$$

In fact for $n = 0$, the moment expansion of the medium behaves like an electric point-dipole as

$$\mathbf{J}^{ED}(\mathbf{r},\omega) = -i\omega\mathbf{p}(\omega)\delta(\mathbf{r}) \tag{8}$$

Here $\mathbf{p}(\omega)$ is the electric dipole moment in the frequency (ω) domain. By means of the dyadic Green's functions $\overleftrightarrow{G}(\mathbf{R};\omega)$ and $\overleftrightarrow{G}^{m}(\mathbf{R};\omega)$, quite simple formulas for the electric ($\mathbf{E}^{ED}(\mathbf{r};\omega)$) and magnetic ($\mathbf{B}^{ED}(\mathbf{r};\omega)$) fields from the electric dipole source can be found as [25]:

$$\begin{aligned}\mathbf{E}^{ED}(\mathbf{r};\omega) &= \mu_0\omega^2\overleftrightarrow{G}(\mathbf{r};\omega).\mathbf{p}(\omega)\\ \mathbf{B}^{ED}(\mathbf{r};\omega) &= c^{-1}\mu_0\omega^2\overleftrightarrow{G}^{m}(\mathbf{r};\omega).\mathbf{p}(\omega),\end{aligned} \tag{9}$$

We assumed that the background medium is a linear time-invariant medium where $\mathbf{D}(\mathbf{r},\omega) = \epsilon_r(\mathbf{r},\omega)\epsilon_0\mathbf{E}(\mathbf{r},\omega)$ and $n(\mathbf{r},\omega) \equiv\ n_1 + in_2 = \sqrt{\epsilon_r(\mathbf{r},\omega)}$ is a complex function. In this study we assume ϵ_r is independent of the positions of the donor or acceptor, i.e., we neglect the influence of these species on the dielectric.

As we can see in Eq. 5, the medium effects are described in terms of the frequency-dependent macroscopic relative permittivity, $\epsilon_r = \epsilon/\epsilon_0$. Moreover, the screening contribution ϵ_r^{-1} and the local field factor $(\epsilon_r+2)/3$ have also been included in our Green's function. This extra factor in Eq. 5 is important for a homogeneous medium when the dielectric medium is in direct contact with the dipole, but it can be ignored if the donor and acceptor are separated from, for instance, gold nanostructures in vacuum. Indeed, we need to carefully and correctly incorporate local field effects associated with nanostructures that are not in direct contact with the donor and acceptor.

Including the first-order moment of the current density distribution (n=1) which is related to the symmetric and antisymmetric parts of the tensorial terms in Eq. 6 we obtain:

$$\mathbf{J}^{1}(r,t) = -\mathbf{J}^{MD+EQ}(t).\nabla\delta(\mathbf{r}) \tag{10}$$

The fields generated by the magnetic dipole current density $\mathbf{m}$ are defined as

$$\begin{aligned}\mathbf{B}^{MD}(\mathbf{r};\omega) &= c^{-2}\mu_0\omega^2\overleftrightarrow{G}(\mathbf{r};\omega).\mathbf{m}(\omega)\\ \mathbf{E}^{MD}(\mathbf{r};\omega) &= -c^{-1}\mu_0\omega^2\overleftrightarrow{G}^{m}(\mathbf{r};\omega).\mathbf{m}(\omega).\end{aligned} \tag{11}$$

The electric field and the magnetic field from an electric quadrupole source are given by

$$\begin{aligned}\mathbf{E}^{EQ}(\mathbf{r},\omega) &= -\mu_0\omega^2\overleftrightarrow{Q} : \nabla\overleftrightarrow{G}(\mathbf{r},\omega)\\ \mathbf{B}^{EQ}(\mathbf{r},\omega) &= -c^{-1}\mu_0\omega^2\overleftrightarrow{Q} : \nabla\overleftrightarrow{G}^{m}(\mathbf{r},\omega)\end{aligned} \tag{12}$$

where Q_{jk} is the electric quadrupole moment tensor defined as $Q_{jk} = \frac{1}{2}\int x'_j x'_k \rho(\mathbf{x}')d^3x'$ and $(\overleftrightarrow{Q} : \nabla\overleftrightarrow{G})_i = \sum_{j,k} Q_{jk}\nabla_k G_{ji}$.

We note that the dyadic Green's function $\overleftrightarrow{G}(\mathbf{r},\omega)$, which describes the fields $E^{ED}(\mathbf{r},\omega)$ and $B^{MD}(\mathbf{r},\omega)$ from electric and magnetic dipoles, has terms that depend on r^{-1}, r^{-2}, and r^{-3}. However, the near-zone term is missing for the fields $B^{ED}(\mathbf{r},\omega)$ and $E^{MD}(\mathbf{r},\omega)$, because these fields are defined by the Green's function $\overleftrightarrow{G}^m(\mathbf{r};\omega)$, which only has r^{-1} and r^{-2} terms.

On the other hand, the electric and magnetic fields from a quadrupole current density source are characterized by the tensors $\nabla\overleftrightarrow{G}(\mathbf{r};\omega)$ and $\nabla\overleftrightarrow{G}^M(\mathbf{r};\omega)$, respectively. Therefore, $\mathbf{E}^{EQ}(\mathbf{r},\omega)$ has terms varying as r^{-1}, r^{-2}, r^{-3}, and r^{-4}. A term with a r^{-4} distance dependence is not present in $\mathbf{B}^{EQ}(\mathbf{r},\omega)$.

Assume that a single radiating donor is placed at $\mathbf{r}_D$, and that the donor size is comparable with the distance between donor and acceptor. We introduce the relationship between the electric and magnetic fields generated by a donor and the dyadic Green's function. The total electric field in our system is the sum of the E-field of the electric dipole ($\mathbf{E}^{ED}$), the E-field of the magnetic dipole ($\mathbf{E}^{MD}$), and the E-field of the electric quadrupole ($\mathbf{E}^{EQ}$), while the total magnetic field is the sum of the M-field of the electric dipole ($\mathbf{B}^{ED}$), the M-field of the magnetic dipole ($\mathbf{B}^{MD}$), and the M-field of the electric quadrupole ($\mathbf{B}^{EQ}$):

$$\mathbf{E} = \mathbf{E}^{ED} + \mathbf{E}^{MD} + \mathbf{E}^{EQ} \tag{13}$$

$$\mathbf{B} = \mathbf{B}^{ED} + \mathbf{B}^{MD} + \mathbf{B}^{EQ}. \tag{14}$$

We should note that dipole-allowed transitions are caused by the electric field of the radiation acting uniformly through the molecular volume while quadrupole transitions are caused by spatial variation in the field. Thus the electric quadrupole as a second rank tensor interacts with the gradient of the electric field defined as

$$\nabla\mathbf{E} = \nabla\mathbf{E}^{ED} + \nabla\mathbf{E}^{MD} + \nabla\mathbf{E}^{EQ}. \tag{15}$$

Knowing that for absorbing and dispersive media, in the framework of quantum electrodynamics and Fermi's Golden rule, the transition matrix element with only the electric dipole-electric dipole interaction included is expressed as [27–30]:

$$M = -\mu_0\omega^2\mathbf{P}_A.\overleftrightarrow{G}(\mathbf{r}_A,\mathbf{r}_D,\omega).\mathbf{P}_D \tag{16}$$

where $\mathbf{P}_{D(A)}$ is the vector of the transition dipole moment of the donor (acceptor). However, by including the interaction of magnetic dipole and electric quadrupole, the matrix element

becomes more complicated:

$$\begin{aligned} M^{E_{d,m,q}}(\mathbf{r}_A,\mathbf{r}_D,\omega) &= -\mu_0\omega^2\mathbf{p}_A\cdot\Big[(\overleftrightarrow{G}\cdot\mathbf{p}_D)-(\overleftrightarrow{G}^m\cdot\frac{\mathbf{m}_D}{c})-(\overleftrightarrow{Q}_D:\nabla\overleftrightarrow{G})\Big] \\ M^{B_{d,m,q}}(\mathbf{r}_A,\mathbf{r}_D,\omega) &= -\mu_0\omega^2\frac{\mathbf{m}_A}{c}\cdot\Big[(\overleftrightarrow{G}^m\cdot\mathbf{p}_D)-(\overleftrightarrow{G}\cdot\frac{\mathbf{m}_D}{c})+(\overleftrightarrow{Q}_D:\nabla\overleftrightarrow{G}^m)\Big] \\ M^{\nabla E_{d,m,q}}(\mathbf{r}_A,\mathbf{r}_D,\omega) &= -\mu_0\omega^2\overleftrightarrow{Q}_A:\Big[\nabla(\overleftrightarrow{G}\cdot\mathbf{p}_D)-\nabla(\overleftrightarrow{G}^m\cdot\frac{\mathbf{m}_D}{c})-\nabla(\overleftrightarrow{Q}_D:\nabla\overleftrightarrow{G})\Big] \end{aligned} \tag{17}$$

and the total matrix element is given by:

$$\mathcal{M} = M^{E_{d,m,q}}(\mathbf{r}_A,\mathbf{r}_D,\omega)+M^{B_{d,m,q}}(\mathbf{r}_A,\mathbf{r}_D,\omega)+M^{\nabla E_{d,m,q}}(\mathbf{r}_A,\mathbf{r}_D,\omega). \tag{18}$$

Comparing elements of the tensors in Eq. 18 with Eq. S1,Eq. S2,Eq. S3, and using the corresponding expressions for the EM and ME coupling term from [29], we obtain the final form of the transition matrix based on the response fields at $\mathbf{r}_A$ (the position of the acceptor) caused by the donor as

$$\begin{aligned} M^{E_{d,m,q}}(\mathbf{r}_A,\mathbf{r}_D,\omega) &= -\mathbf{p}_A(\mathbf{r}_A).\left[\mathbf{E}^{ED}(\mathbf{r}_A,\omega)+\mathbf{E}^{MD}(\mathbf{r}_A,\omega)+\mathbf{E}^{EQ}(\mathbf{r}_A,\omega)\right] \\ M^{B_{d,m,q}}(\mathbf{r}_A,\mathbf{r}_D,\omega) &= -\mathbf{m}_A(\mathbf{r}_A).\left[\mathbf{B}^{ED}(\mathbf{r}_A,\omega)+\mathbf{B}^{MD}(\mathbf{r}_A,\omega)+\mathbf{B}^{EQ}(\mathbf{r}_A,\omega)\right] \\ M^{\nabla E_{d,m,q}}(\mathbf{r}_A,\mathbf{r}_D,\omega) &= -\overleftrightarrow{Q}_A(\mathbf{r}_A):\left[\nabla\mathbf{E}^{ED}(\mathbf{r}_A,\omega)+\nabla\mathbf{E}^{MD}(\mathbf{r}_A,\omega)+\nabla\mathbf{E}^{EQ}(\mathbf{r}_A,\omega)\right] \end{aligned} \tag{19}$$

These expressions provide intuitive generalizations of Eq. 8 for determining the interactions between different multipoles with the electromagnetic fields generated by another set of multipoles (details of the derivation of this set of equations can be found in the SI).

Note that in the derivation of Eq. 19, second order tensors arise from the dyadic product of two vectors, $\mathbf{a}$ and $\mathbf{b}$

$$\overleftrightarrow{S} = \mathbf{a}\otimes\mathbf{b} \qquad S_{ij} = a_i b_j. \tag{20}$$

and as a result, if S and T are two second order tensors, the inner product of S and T is a scalar, denoted by $\overleftrightarrow{S}:\overleftrightarrow{T}$, represented by their components:

$$\overleftrightarrow{S}:\overleftrightarrow{T} = S_{ij}T_{ij}. \tag{21}$$

Eq. 19 includes the effect from both electric and magnetic fields, as well as the electric field gradient. The gradient of the field,$\nabla\mathbf{E}$, contains nine components, e.g. $(\nabla\mathbf{E})_{\beta\gamma}$ is the change of the E_β component in the γ direction.

Note that, if there is no DC magnetic field interacting with the system, the dynamics of the system preserve time-reversal symmetry, and all molecular eigenfunctions can be chosen to be real [31]. From this the electric dipole and electric quadrupole transition matrix elements are real, and magnetic dipole transition matrix elements are entirely imaginary [32].

Recasting Eq. 19, the transition matrix based on the fields from the donor at the position of the acceptor is expressed as follows [23, 33]

$$\mathcal{M}(\mathbf{r}_A, \mathbf{r}_D, \omega) = M^e(\mathbf{r}_A, \mathbf{r}_D, \omega) + M^m(\mathbf{r}_A, \mathbf{r}_D, \omega) + M^q(\mathbf{r}_A, \mathbf{r}_D, \omega), \tag{22a}$$

$$\begin{aligned} M^e(\mathbf{r}_A, \mathbf{r}_D, \omega) &= M^{ee} + M^{em} + M^{eq} \\ &= -\mu_A^{eg} \mathbf{e}_A^{\mu} \cdot \left[\frac{\mu_D^{ge}}{p(\omega)} \mathbf{E}^{ED} + \frac{m_D^{ge}}{m(\omega)} \mathbf{E}^{MD} + \frac{q_D^{ge}}{q(\omega)} \mathbf{E}^{EQ} \right], \end{aligned} \tag{22b}$$

$$\begin{aligned} M^m(\mathbf{r}_A, \mathbf{r}_D, \omega) &= M^{me} + M^{mm} + M^{mq} \\ &= -m_A^{eg} \mathbf{e}_A^{m} \cdot \left[\frac{\mu_D^{ge}}{p(\omega)} \mathbf{B}^{ED} + \frac{m_D^{ge}}{m(\omega)} \mathbf{B}^{MD} + \frac{q_D^{ge}}{q(\omega)} \mathbf{B}^{EQ} \right], \end{aligned} \tag{22c}$$

$$\begin{aligned} M^q(\mathbf{r}_A, \mathbf{r}_D, \omega) &= M^{qe} + M^{qm} + M^{qq} \\ &= -q_A^{eg \overleftrightarrow{e}^q} : \left[\frac{\mu_D^{ge}}{p(\omega)} \nabla \mathbf{E}^{ED} + \frac{m_D^{ge}}{m(\omega)} \nabla \mathbf{E}^{MD} + \frac{q_D^{ge}}{q(\omega)} \nabla \mathbf{E}^{EQ} \right]. \end{aligned} \tag{22d}$$

Eq. 22 enables the study of resonance energy transfer in inhomogeneous, absorbing, and dispersive media for the cases where the sizes of the donor and the acceptor are comparable to the distance between them. Note that the pre-factors in front of each $\mathbf{E}$ and $\nabla\mathbf{E}$ is for renormalization so that the fields have the correct magnitudes, corresponding to the donor transition multipole moments.

Considering the size of donor/acceptor to be d ($d \ll \lambda$) and $d \leqq R$, eight additional terms, due to the contribution of magnetic dipole and electric quadrupole, are included in the RET rate calculation, as compared to the traditional Förster formulation. The rate of RET can then be determined by substituting M^{ee} in Eq. 2 with the new form of the transition matrix element presented in Eq. 22.

The necessary condition of the multipole expansion to be useful is that the transition density distributions of the interacting molecules do not overlap, i.e., the inter-chromophore separation $R \geqslant (r_D + r_A)$ where $r_{D/A}$ is the radius of the donor or acceptor. Note that transition selection rules often make some of the transition multipoles vanish, causing certain terms in Eq. 22 to be zero. In general, the selection rules for $\mathbf{m}^{km}$ and $\mathbf{q}^{km}$ can be different

from that for the electric dipole, and therefore give non-zero transitions between two states even when the dipole transition is forbidden.

III. RESULTS AND DISCUSSION

Here we explicitly examine the total coupling intensity, $|M|^2$, for selected situations to provide better insight about the role of the different terms. $|M|^2$ includes both purely electric, magnetic and quadrupole contributions to the transfer matrix element in addition to interference terms corresponding to mixed electric-magnetic, electric-quadrupole and magnetic-quadrupole couplings as follows

$$|\mathcal{M}|^2 = |M^{ee} + M^{mm} + M^{qq} + (M^{em} + M^{me}) + (M^{eq} + M^{qe}) + (M^{mq} + M^{qm})|^2 \tag{23}$$

Although Eq. 23 seems very complicated, we may simplify it with an initial consideration of the geometry and transition moment symmetry of the donor and acceptor. The next few paragraphs provides a general consideration of simplifications that can arise, and then we provide numerical results for simple model systems that include electric quadrupole and magnetic dipole effects. All these examples refer to donors and acceptors in a homogeneous medium; in the future we will examine the influence of plasmonic particles present in the medium on donor-acceptor energy transfer when electric quadrupole and magnetic dipole effects are important.

Generally, the interaction between molecules with sufficiently low symmetry and no proper axis of rotation (chiral or optically active molecules), are dominated by the electric dipole terms for resonance energy transfer. However this type of molecule is also subject to additional small interactions which are different for left handed-left handed as opposed to left handed-right handed enantiomer combinations. For a discussion of intermolecular interactions between optically active molecules, the contributions from magnetic-magnetic dipole and also electric-magnetic dipole must be taken into account. These contributions come from the magnetic transition dipole connecting the excited(ground) state of donor(acceptor) to its ground(excited) state, when both of them are allowed. The condition is met if the donor is chiral but not when it is centrosymmetric. Thus the theory we have developed could be useful for comparing energy in chiral assemblies of molecules compared to a racemic mixture of the same molecules, as has been examined by Rodriguez and Salam [34]

Thus the theory we have developed could be useful for comparing energy in chiral assemblies of molecules compared to a racemic mixture of the same molecules.

On the other hand, due to importance of the orientation of the electric and magnetic dipoles in donor/acceptor, there can be orientations where there is no energy transfer for optically active species. It is not hard show from Eq. 22 that when $\mu^D \parallel m^A$ and $m^D \parallel \mu^A$, the energy transfer matrix elements (M^{em} and M^{me}) are zero even though the transition dipoles are nonzero, as previously noted.[29, 32] However, the total energy transfer rate could survive due to other interactions, such as electric dipole-electric dipole coupling (M^{ee}), or magnetic dipole-magnetic dipole coupling (M^{mm}), etc. We will discuss this in case 4 of the numerical section in more detail.

It should be noted that the magnetic dipole transition moment amplitude is smaller (for molecules smaller than a few nm) than the electric dipole transition moment by two to three orders of magnitude, i.e., $M^{mm}/M^{ee} \leqslant 10^{-3}$ and if the leading contribution is coming from the electric-electric dipole coupling, the amplitude of magnetic dipole transitions both in donor and acceptor can be discarded ($|M^{mm}|^2 \approx 0$) [29, 32, 35, 36]. Magnetic quadrupole and higher magnetic multipoles should also be negligible in this situation. However we note that for large nanoparticle structures, it is possible to have magnetic and electric transition moments that are comparable in size, in which case the terms in Eq. 22 would need to be fully evaluated to generate accurate results [37]

In the near zone limit, it has been shown that the electric quadrupole-quadrupole and magnetic dipole-electric quadrupole interactions are small [35, 38]. This is also apparent in Eq. 22 when one examines the distance dependence of the relevant quadrupole fields in comparison with the corresponding dipole fields. However generally the coupling of magnetic dipole-electric quadrupole is nonzero for oriented molecular pairs but vanishes on rotational averaging if we consider an ensemble of randomly oriented molecules [35, 39, 40]

We may identify further simplifications to Eq. 23 by looking at the contribution of electric dipole-quadrupole interference terms; M^{eq}, M^{qe}. These two interference terms cancel for an ordered ensemble with the same orientation and same magnitude for electric dipole and quadrupole transitions for both donor and acceptor i.e. $M^{eq} + M^{qe} = 0$ [35, 41] (see also SI for proof). This means regardless of donor-acceptor geometry or polarization directions, the electric dipole-electric quadrupole energy transfer vanishes for an ordered system (we also discuss this in case 2 in the simulation section). However, we should be cautious when

treating disordered systems, since orientation averaging should be employed to determine the total energy transfer rate.

Numerical simulation

To illustrate the effect of including transition magnetic dipole and electric quadrupole, we calculate the distance-dependent coupling intensity for different cases in which different multipoles are considered for donor and acceptor, and show that the coupling intensity can be diminished by different types of interferences. The matrix element (coupling intensity) in Eq. 23 is determined by the interaction between the acceptor multipoles and the total electric and magnetic fields from the donor. Compared to the electric dipole-dipole approximation, the total fields from the donor are much more complicated, giving rise to interferences in the fields and the multipole-field interactions. More specifically, interferences can come from two origins: the interferences between the fields generated by different donor multipoles, and the cancellation of interaction energies between different acceptor multipole-donor field interactions.

In the following sections, we analyze the electric dipole-electric quadrupole (ED-EQ) interference and the electric dipole-magnetic dipole (ED-MD) interference. Using three different ED-EQ cases, we show, respectively, three consequences due to interference, namely: (1) there can be minima in electric field and field gradient magnitudes for certain acceptor locations; (2) there can be cancellation in the contribution to the energy transfer rate that arises from dipole-field and quadrupole-field gradient contributions; and (3) there are modified field orientation effects compared to the dipole only case. Each consequence leads to a dip in the coupling intensity at a certain donor-acceptor distance. On the other hand, the ED-MD case provides an example where the energy transfer rate is completely suppressed, regardless the donor-acceptor separation, due to the ED-MD interference.

A total of four cases will be discussed, with various donor-acceptor configurations and multipoles. The simulations are performed with spatial distributions of the donor and acceptor shown in Fig. 1 (a) or (b). The donor is centered at the origin, with the donor-acceptor pair axis aligned with the x-axis. Spheres are used to represent the two particles, but the orientations of multipoles may vary in each case. If the acceptor is located on the positive side of the x-axis, the configuration is named Side A; otherwise, Side B. In either configuration,

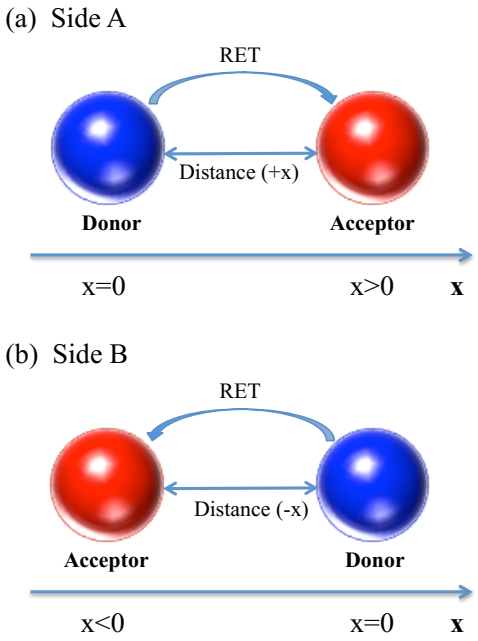

FIG. 1. Schematic representation of the system considered in the simulation. The donor is located at the origin of the coordinate system, while the acceptor is placed either on the positive x-axis (Side A) or on the negative x-axis (Side B).

the distance is defined as the absolute distance between the donor and the acceptor.

Case 1: Electric dipole-electric quadrupole (ED-EQ) interference - field magnitude minimum

The first case in our analysis is to show that the interference between the donor dipole field and donor quadrupole field can create local minima in the total field intensity, as well as the total field gradient intensity, leading to large suppression of donor-acceptor electronic coupling with a certain particle separation. This case uses Fig. 1(a) as its configuration, with well defined transition electric dipole and quadrupole moments associated with the donor and the acceptor. The fields generated by these multipoles lead to destructive interference along the positive x-axis, giving rise to a dip in the donor-acceptor coupling intensity.

The donor and acceptor multipoles are defined as the following. The donor electric dipole is assumed to point towards the positive y-axis with a magnitude of 1 Debye, i.e. $\mu_1 = (0, 1, 0)$ D. The donor quadrupole emitter consists of 4 point charges in the xy-plane. Each charge has a magnitude of $2.082e$, and is located in one quadrant of the plane, at a

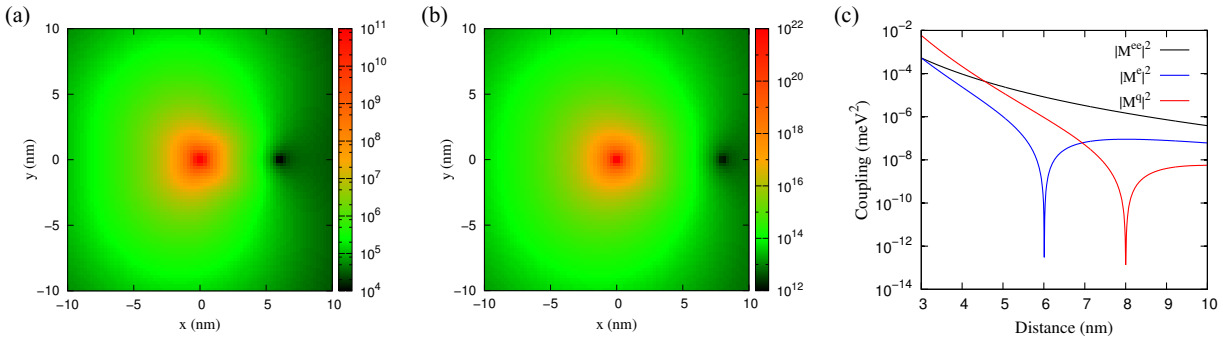

FIG. 2. Heat maps, for Case 1, of the magnitude of the total electric field ($\mathbf{E}^{tot}$) (a) and the magnitude of the gradient of the total electric field ($\nabla\mathbf{E}^{tot}$) (b) in the xy-plane with $z = 0$ nm. (c) The coupling intensity associated with an acceptor having an electric dipole-field interaction or an electric quadrupole-field gradient interaction.

distance of 0.5 Å along each axis (x and y). The charges in the first and the third quadrants are negative, while the other two are positive. This charge distribution gives an electric quadrupole tensor with all zero matrix elements except $Q_{12} = Q_{21} = -10$ D·Å. Both the dipole and the quadrupole are oscillating with a frequency of 475.86 THz (equivalent to 630 nm). In order to separate the effects of the total field and the total field gradient, two acceptors are considered here: one with the same electric dipole as the donor but no quadrupole, and the other with the same quadrupole as the donor but no dipole. Hence, the first acceptor would interact with the electric fields only, while the second only interacts with the field gradients. Note that only one acceptor is coupled with the donor at one time, not both at the same time. The magnetic dipole in this case is assumed to be zero for both the donor and the acceptors.

The total electric field magnitude (where $\mathbf{E}^{tot} = \mathbf{E}^{ED} + \mathbf{E}^{EQ}$) associated with the donor dipole and quadrupole transition moments as defined is presented in Fig. 2(a), while Fig. 2(b) shows the magnitude of the total field gradient ($\nabla\mathbf{E}^{tot}$). It is obvious that there is a minimum along the positive x-axis in each heat map. The minimum in the field map (Fig. 2(a)) is caused by interference between the donor field and the quadrupole field, which can be seen in the corresponding vector maps of the fields in the xy-plane (see Fig. S1 in SI). The vector maps plot the real parts of the x and y components of the different fields, while their corresponding imaginary parts at these distances are several orders of magnitudes smaller.

Because we assume that the acceptor has the same orientation as the donor, together with the fact that the electric fields interact with the dipole moment of the acceptor via a dot product operation, only the y components of the fields can affect the coupling strength. Therefore, there is no need to analyze the z components of the electric fields in Case 1.

In Fig. S1 (a) and (b), the electric fields from the dipole and the quadrupole have the conventional vector maps, while a local minimum can be observed in the total field (Fig. S1(c)). The dipole field has two symmetrical loops on the positive and negative sides of x-axis, while the quadrupole field has four loops, one in each quadrant of the xy-plane. The quadrupole field is stronger than the dipole field near the origin, but decays more rapidly as distance increases. Because of the nature of the field lines, the total field along the positive x-axis is affected by the destructive interference between the dipole and quadrupole fields. This interference causes a minimum at $x = 6$ nm, while the quadrupole and dipole fields dominate at positions before and after 6 nm, respectively. The gradient of the fields have a more complicated pattern, although the origin of the local minimum is coming from the same effect, as shown in Fig. S2. The field gradient vector plots present only the xy and yx components of the gradients, because those components are the only non-zero elements in the selected quadrupole tensor.

Due to the local minima in $\mathbf{E}^{tot}$ and $\nabla\mathbf{E}^{tot}$, and given that the prefactors to these fields in Eq. 22b (i.e., $\mu_D^{ge}/p(\omega)$ and $q_D^{ge}/q(\omega)$) are comparable in magnitude, it is expected to see dips in the coupling intensities ($|M^e|^2$ and $|M^q|^2$), and therefore in the resonance energy transfer rate. Indeed, Fig. 2(c) shows a dip in both types of coupling, namely the coupling between the acceptor dipole moment and the total field from the donor ($|M^e|^2$), and the coupling between the acceptor quadrupole and the gradient of the donor fields ($|M^q|^2$). The dipole-dipole coupling (green line) is a smoothly decaying line as expected, since the dipole field without interference decays smoothly (as $1/R^3$) and the acceptor dipole is aligned with the donor's.

Case 2: ED-EQ interference - interaction energy cancellation

Using the Side B configuration in Fig. 1(b), we investigate the second case mentioned earlier, in which there is cancellation of interaction energies between the dipole-field and quadrupole-field gradient interactions, resulting in a suppression in the donor-acceptor cou-

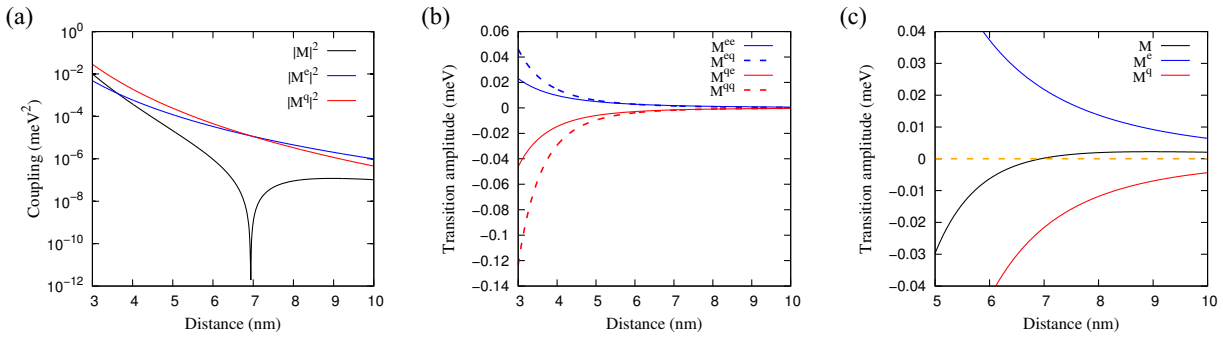

FIG. 3. The coupling intensity (a) and transition amplitude (b, c) for different multipole interactions for Case 2. Plots of the transition amplitudes (b, c) only show the real parts. The orange dashed line in (c) marks the value of zero for easy observation.

pling intensity. The transition multipoles for the donor and the acceptor are kept the same as defined in Case 1, except that the acceptor has both dipole and quadrupole moments. The Side B configuration shows a smoothly decaying electric field and field gradient (Fig. 2(a) and (b)), without any local minimum. Usually, this suggests that, provided the acceptor multipoles being the same as the donor's, the coupling intensity decays smoothly as the donor-acceptor distance increases. This is indeed the case for $|M^e|^2$ and $|M^q|^2$ (see blue and red lines in Fig. 3(a), respectively), which are calculated using Eq. 22b and Eq. 22d, respectively. However, the total coupling intensity ($|\mathcal{M}|^2 = |M^e + M^q|^2$, black line) clearly shows a dip close to $x = -7\,\text{nm}$ (distance 7 nm).

The dip in coupling intensity $|\mathcal{M}|^2$ is not due to destructive interference in the field or field gradient, but in fact, comes from cancellation between the interaction energies of the dipole and the quadrupole with the fields and the field gradients, respectively. In other words, in contrast to Case 1 where the cancellation occurs within Eq. 22b or 22d, it happens between these two equations. In Fig. 3(b), one can see that the transition amplitudes from the $\mathbf{p}_A$-$\mathbf{E}_D^{ED}$ interaction (M^{ee}) and the $\mathbf{p}_A$-$\mathbf{E}_D^{EQ}$ interaction (M^{eq}) are both positive, while the $\overleftrightarrow{Q}_A$-$\nabla\mathbf{E}_D^{ED}$ (M^{qe}) and $\overleftrightarrow{Q}_A$-$\nabla\mathbf{E}_D^{EQ}$ (M^{qq}) interactions are both negative. When summing over all interactions in Eq. 22a, the total transition amplitude $\mathcal{M}$ (Fig. 3(c) black line) passes through zero when $x = -7\,\text{nm}$ and a local minimum in the coupling intensity $|\mathcal{M}|^2$ appears. Therefore, it is not always possible to predict the behavior of the coupling intensity by considering only the magnitudes of the total electric field and field gradient.

The interactions between the acceptor multipoles and the donor fields and field gradients must be analyzed before reaching any conclusion for the energy transfer rate.

It is worth noting that only the real part of the transition amplitudes are plotted in Fig. 3 (b, c), which could reach zero at a certain distance. On the other hand, the imaginary part of $\mathcal{M}$, although small at most distances, may not be exactly zero. Hence, even though at a distance of 7 nm, the real part of $\mathcal{M}$ is zero, the total coupling intensity term ($|\mathcal{M}|^2$) still has a non-zero residual value.

Case 3: ED-EQ interference - modified field orientation

Analysis of Case 3 shows that the ED-EQ interference can also lead to a modified total field orientation, as compared to the pure dipole field, giving rise to a misalignment between the acceptor multipoles and the donor fields and field gradients. In this case, the multipole moments of the donor and the acceptor are the transition dipole and quadrupole moments of the first excited state of a 512-atom PbS quantum dot.[42] The transition dipole has the form $\boldsymbol{\mu}^{\mathrm{PbS}} = (0.116, 0.848, 0.049)$ D, while $\overleftrightarrow{Q}^{\mathrm{PbS}}$ (in unit of D·Å) is defined by the following tensor elements: $Q_{11} = 1.968$, $Q_{22} = -4.039$, $Q_{33} = 2.070$, $Q_{12} = Q_{21} = 6.484$, $Q_{13} = Q_{31} = -0.080$, and $Q_{23} = Q_{32} = 1.581$. The wavelength of the donor emission is at 630 nm. The donor and the acceptor are assumed to have the same identity and orientation.

Fig. 4(a) shows the coupling intensities associated with different multipole interactions, as well as the total coupling summing over all interactions (using Eq. 22a), which exhibits different characteristics at short, intermediate, and long range distances. First, the total coupling ($|\mathcal{M}|^2$, black line) at short distance (< 3.5 nm) is larger than the dipole-dipole coupling ($|M^{ee}|^2$, green line), due to the constructive interference between the $\mathbf{p}_A$-$\mathbf{E}_D$ and $\overleftrightarrow{Q}_A$-$\nabla\mathbf{E}_D$ interactions. Second, $|\mathcal{M}|^2$ converges towards $|M^{ee}|^2$ at large distance because of the dominating dipole field. Third, the coupling intensities have local minima at certain distances. Through the following analysis, we shall see that the local minima in $|M^e|^2$ and $|M^q|^2$ are caused by the misaligned interaction between multipole and field/field gradient.

The magnitudes of the total electric field and the field gradient generated by dipole and quadrupole are shown in Fig. S3, in which a dip can be found in the fourth quadrant of the xy-plane. Similar to Case 1, the local minima are caused by interference between the two multipoles (see vector plots for the fields in Fig. S4). However, the dips in the fourth

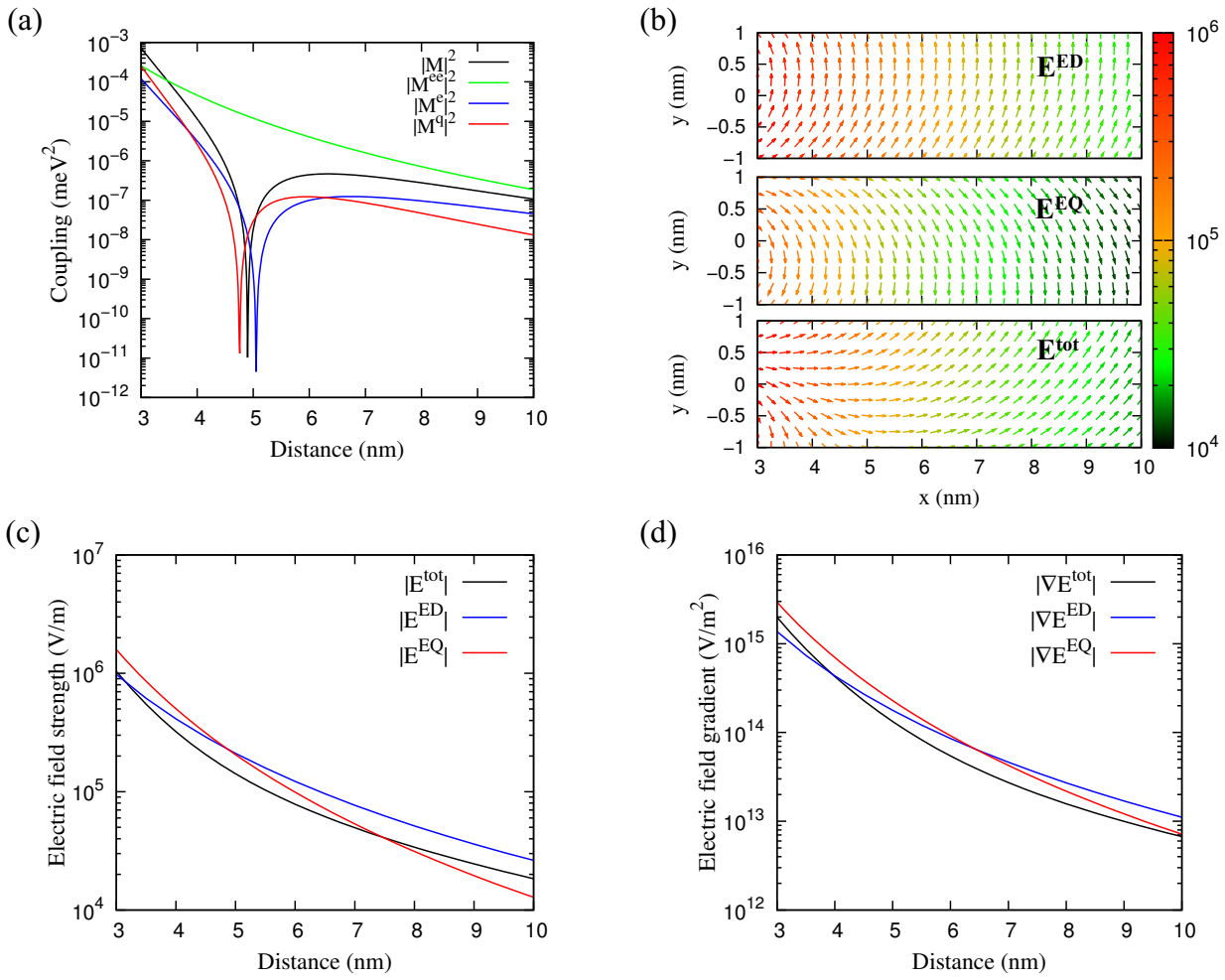

FIG. 4. Coupling intensities, electric fields, and field gradients associated with the different multipoles for Case 3. (a) The coupling intensity of different multipole interactions. (b) Vector plots of the different electric fields, showing the real parts of the x and y components, in the xy plane with $z = 0$ nm. (c) Magnitudes of electric fields along the x-axis. (d) Magnitudes of the field gradients along the x-axis.

quadrant have insignificant effects on the magnitudes of the total field and field gradient on the positive x-axis (Fig. 4(c) and (d)), which have no local minimum at the distances in interest. Meanwhile, by examining the vector plots carefully (Fig. 4(b)), one can see that due to interference, the total electric field ($\mathbf{E}^{tot}$) has an orientation change from $x = 3$ nm to $x = 8$ nm. The field has a significant contribution from the y component between $x = 3$ nm and 4 nm. However, it becomes parallel to x-axis around $x = 5$ nm, which means that at this

distance, the interaction between the field and the acceptor dipole moment (mostly aligned with y-axis) is minimal. Then, the field gradually increases its y component, giving a much larger interaction with the acceptor dipole as compared to that at $x = 4.5$ nm. Hence, the coupling intensity due to the $\mathbf{p}_A$-$\mathbf{E}_D$ interaction ($|M^e|^2$, blue line in Fig. 4(a)) exhibits a dip at $x = 5$ nm. The dip in the coupling of the $\overleftrightarrow{Q}_A$-$\nabla\mathbf{E}_D$ interaction ($|M^q|^2$, red line) has a similar origin. Finally, the dip in the total coupling intensity ($|\mathcal{M}|^2$) comes from the interaction energy cancellation effect as described in Case 2.

The study of different coupling intensities shows the complexity of the interactions among the multipoles. The multipole interference can lead to a local minimum in field magnitude, modification in field orientation, and cancellation of the interaction energy. Any one of the effects could result in a dip in the coupling intensity. Therefore, it is important to analyze the coupling intensity as determined by Eq. 18 instead of the field magnitude alone.

Case 4: Electric dipole-magnetic dipole (ED-MD) interference - total suppression of energy transfer

Electric dipole-magnetic dipole interference is examined in Case 4, where the electric quadrupole moments are set to zero. This means that only Eqs. 22b and 22c would provide non-zero results, rather than Eq. 22d. We find that it is common for the cross terms M^{em} and M^{me} to be zero, due to orthogonality of the electric and magnetic fields from the oscillating electric and magnetic dipoles. It is also possible to orient the dipoles in such a way that the energy transfer is nearly completely turned off.

Fig. 5 shows the distance-dependent coupling intensity ratio using different donor and acceptor magnetic dipoles, while both donor and acceptor electric dipoles are kept at 1 D and aligned with y-axis. Each plot contains two types of ratios: the ratio of total coupling intensity ($|\mathcal{M}|^2$) to the ED-ED coupling ($|M^{ee}|^2$), and the ratio of the sum of ED-ED and MD-MD coupling ($|M^{ee} + M^{mm}|^2$) to the ED-ED coupling ($|M^{ee}|^2$). The difference between them, if any, is from the contributions of the cross terms: the interaction between the electric dipole and the electric field from the oscillating magnetic dipole (M^{em}), and the interaction between the magnetic dipole and the magnetic field from the oscillating electric dipole (M^{me}). Fig. 5(a) and (b) show that if the magnetic dipoles of the donor and the acceptor are both aligned with either x or y axis, together with the y-oriented ED, the cross

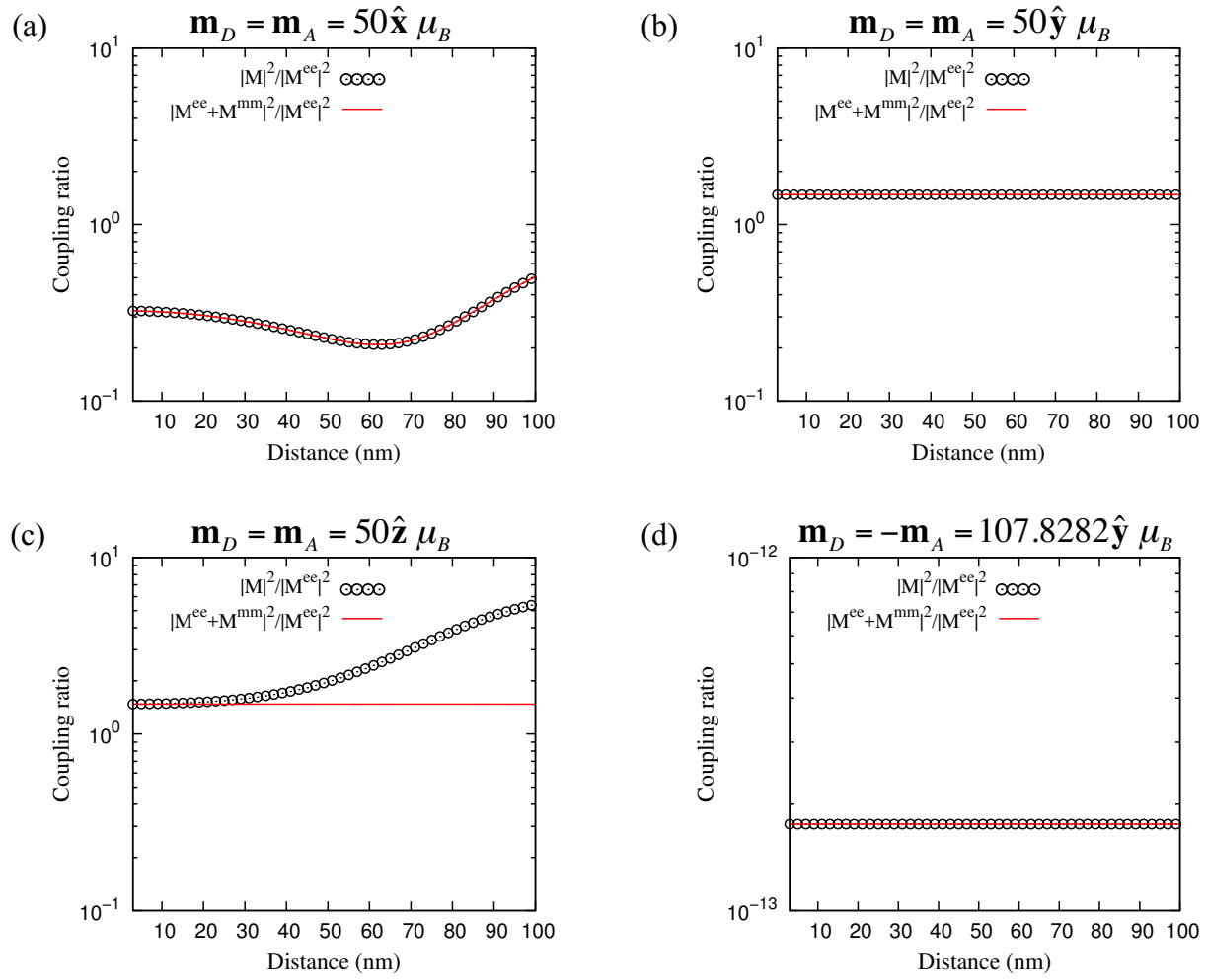

FIG. 5. Coupling intensity ratio for Case 4 with various $\mathbf{m}$ orientations and magnitudes. (a - c) $\mathbf{m}_D = \mathbf{m}_A$ with magnitude of $50\,\mu_B$ (Bohr Magneton) in x direction, y direction, and z direction, respectively. (d) $\mathbf{m}_D = -\mathbf{m}_A$, with magnitude of $107.8282\,\mu_B$. The black circles represent the ratio of the total coupling intensity ($|\mathcal{M}|^2$) to the ED-ED coupling ($|M^{ee}|^2$), while the red line is for the ratio of the sum of ED-ED and MD-MD coupling ($|M^{ee} + M^{mm}|^2$) to the ED-ED coupling ($|M^{ee}|^2$).

terms are zero, and the two types of ratio coincide with each other. When the MDs are both aligned with x-axis the energy transfer rate is suppressed for a wide range of distance, from 3 nm to 100 nm, due to interaction energy cancellation. When the MDs are both in the positive y direction, very small enhancement can be seen.

On the other hand, if the MDs are both aligned with the z-axis, then larger enhancement

in the total coupling intensity can be achieved at large distances ($> 30\,\mathrm{nm}$), as demonstrated by the ratio $|M|^2/|M^{ee}|^2$ (Fig. 5(c)). The deviation between the two ratios in this plot suggests that with for z-oriented magnetic dipoles, the cross terms, from the $\mathbf{p}_A$-$\mathbf{E}_D^{MD}$ and the $\mathbf{m}_A$-$\mathbf{B}_D^{ED}$ interactions, provide a significant contribution, especially at large distances.

In addition, if the MDs of the donor and the acceptor are aligned with y-axis, but pointing towards opposite directions, it is possible to completely turn off the resonance energy transfer by choosing the appropriate MD magnitude. Fig. 5(d) shows that when the magnitude of MD is $107.8282\,\mu_B$ (unit of Bohr Magneton), the coupling ratio remains constant at the value of 10^{-13} when varying the donor-acceptor distance. Note that in order to reach this total suppression, the magnetic dipole magnitude has to be much larger than the electric dipole, when both are expressed in atomic units. The electric dipole magnitude of 1 D equals to 0.3934 atomic units, while the MD magnitude of $107.8282\,\mu_B$ is almost 54 atomic units, i.e. 2 orders of magnitude larger than the electric dipole. This control condition is possible in a nonsymmetric bichromophore system or a layered Langmuir-Blodgett film[36].

IV. CONCLUSION

We have extended Förster theory beyond the dipole approximation by introducing a general but practical computational scheme to simulate RET in inhomogeneous absorbing and dispersive media which can be easily implemented using a real-time electrodynamics approach, the so-called "the time-domain electrodynamics resonance energy transfer" (TED-RET) method. The main focus of this work is on Eq. 22, which allows us to study RET at donor/acceptor separations comparable to the size of the donor or acceptor for an arbitrary dielectric medium that could include plasmonic particles. The formulas also take care of energy transfer when the electric dipole transitions are forbidden, which was an important missing aspect of our previous work. Comparing with the general FRET approach in which only the electric dipole is included, we have a much more complicated transition matrix element, although the form is conceptually straightforward, and we have therefore been able to use it in numerical applications. These applications have demonstrated the usefulness and capability of our new formulation by examining energy transfer simulations for different cases of multipole resonance configurations with a complex spatial distribution of matrix elements. Using a toy model and 512-atom lead sulfide (PbS) quantum dot, we found that the following

effects can play a role in energy transfer: (1) there can be a minimum in energy transfer rates that arises from interfering electric field and field gradients; (2) there can be cancellation of interaction energies associated with dipole-field and quadrupole-field gradients; and (3) higher multipoles lead to modified field orientation compared to the dipole only case. As a last part of the numerical simulation, the electric dipole-magnetic dipole interference is discussed in detail. The results demonstrate important deviations from conventional rate calculations using Förster theory, and we have also set the stage for properly and efficiently implementing plasmon coupled (PC)-RET calculations in relatively large particles that are important in biology, optical switching, solar cells, where energy transfer processes typically take place in inhomogeneous absorbing and dispersive media.

ACKNOWLEDGMENTS

This work was supported by the U.S. National Science Foundation under Grant No. CHE-1465045. The authors would also like to thank Mohamad S. Kodaimati for providing the TD-DFT simulation results for the 512-atom lead sulfide quantum dot.This research was supported in part through the computational resources and staff contributions provided for the Quest high performance computing facility at Northwestern University which is jointly supported by the Office of the Provost, the Office for Research, and Northwestern University Information Technology.

[1] T. Förster, Ann. Physik. **2**, 55 (1948).

[2] L. Stryer and R. P. Haugland, Proc. Natl. Acad. Sci. U.S.A. **58**, 719725 (1967).

[3] Y. Chen, M. B. O'Donoghue, Y.-F. Huang, H. Kang, J. A. Phillips, X. Chen, M. Carmen Estevez, C. J. Yang, and W. Tan, J. Am. Chem. Soc. **132**, 16559 (2010).

[4] M. P. Jennings, T. L.; Singh and G. F. Strouse, J. Am. Chem. Soc. **128**, 5462 (2006).

[5] A. K. Singh, S. A. Khan, Z. Fan, T. Demeritte, D. Senapati, R. Kanchanapally, and P. Chandra Ray, J. Am. Chem. Soc **134**, 8662 (2012).

[6] H. Park, N. Heldman, P. Rebentrost, L. Abbondanza, A. Iagatti, A. Alessi, B. Patrizi, M. Salvalaggio, L. Bussotti, and M. Mohseni, Nat. Mater **15**, 211 (2016).

[7] D. Sikdar, W. Cheng, and P. M., J. Appl. Phys. **117**, 083101 (2015).

[8] C. Rupasinghe, I. D. Rukhlenko, and M. Premaratne, ACS Nano **8**, 2431 (2014).

[9] C. Jayasekara, M. Premaratne, M. I. Stockman, and S. D. Gunapala, J. Appl. Phys. **118**, 173101 (2015).

[10] S. Chatterjee, J. B. Lee, N. V. Valappil, D. Luo, and V. M. Menon, Bio. Opt. Express **2**, 1727 (2011).

[11] S. Lu, Z. Lingley, T. Asano, H. D., S. Barwicz, T.and Guha, and A. Madhukar, Nano Lett. **9**, 4548 (2009).

[12] K. Shankar, X. Feng, and C. A. Grimes, ACS Nano **3**, 788 (2009).

[13] D. L. Andrews, Phys. Rev. Lett. **99**, 023601 (2007).

[14] X. Liu and J. Qiu, Chem. Soc. Rev. **44**, 8714 (2015).

[15] M. E. Madjet, A. Abdurahman, and T. Renger, J. Phys. Chem. B **110**, 17368 (2006).

[16] B. P. Krueger, G. D. Scholes, and G. R. Fleming, J. Phys. Chem. B **102**, 5378 (1998).

[17] W. J. D. Beenken and T. Pullerits, J. Chem. Phys. **120**, 2490 (2004).

[18] C. Kagan, C. Murray, M. Nirmal, and B. Bawendi, Phys. Rev. Lett. , 1517 (1996).

[19] G. D. S. R. D. Harcourt and K. P. Ghiggino, J. Chem. Phys. **101**, 10521 (1994).

[20] B. P. Krueger, G. D. Scholes, and G. R. Fleming, J. Phys. Chem. B **102**, 5378 (1998).

[21] A. Muñoz Losa, C. Curutchet, B. Krueger, and H. L. R. M. B., Biophysical Journal **96**, 4779 (2009).

[22] P. López-Tarifa, N. Liguori, N. van den Heuvel, R. Croce, and L. Visscher, Physical Chemistry Chemical Physics **19**, 18311 (2017).

[23] W. Ding, L.-Y. Hsu, and G. C. Schatz, The Journal of Chemical Physics **146**, 064109 (2017).

[24] L.-Y. Hsu, W. Ding, and G. C. Schatz, J. Phys. Chem. Lett. **8**, 2357 (2017).

[25] O. Keller, *Quantum Theory of Near-Field Electrodynamics* (Springer, 2011).

[26] G. Juzelinas and D. L. Andrews, Phys. Rev. B **49**, 8751 (1994).

[27] S. Scheel and S. Y. Buhmann, acta physica slovaca **58**, 675 (2008).

[28] J. A. Crosse and S. Scheel, PHYSICAL REVIEW A **79**, 062902 (2009).

[29] D. L. Andrews and D. S. Bradshaw, Eur. J. Phys. **25**, 845 (2004).

[30] G. D. Scholes and D. L. Andrews, The Journal of Chemical Physics **107**, 5374 (1997).

[31] P. Atkins and R. Friedman, *Molecular Quantum Mechanics* (Oxford University Press, Oxford).

[32] N. Yang and A. E. Cohen, J. Phys. Chem. B **115**, 5304 (2011).

[33] H. T. Dung, L. Knll, and D. G. Welsch, Phys. Rev. A **65**, 043813 (2002).

[34] J. J. Rodriguez and A. Salam, J. Phys. Chem. B **115**, 51835190 (2011).

[35] G. D. Scholes, A. H. A. Clayton, and K. P. Ghiggino, The Journal of Chemical Physics **97**, 7405 (1992).

[36] J. D. Gareth, D. J. Robert, D. S. Bradshaw, and D. L. Andrews, The Journal of Chemical Physics **119**, 2264 (2003).

[37] M. R. Bourgeois, A. T. Liu, M. B. Ross, J. M. Berlin, and G. C. Schatz, The Journal of Physical Chemistry C **121**, 15915 (2017).

[38] D. L. Andrews and B. S. Sherborne, The Journal of Chemical Physics **86**, 4011 (1987).

[39] S. Bernadotte, A. J. Atkins, and C. R. Jacob, The Journal of Chemical Physics **137**, 204106 (2012).

[40] L. D. Barron, *Molecular Light Scattering and Optical Activity* (Cambridge University Press,Cambridged).

[41] E. A. Power and T. Thirunamachandran, The Journal of Chemical Physics **60**, 3695 (1974).

[42] M. S. Kodaimati, C. Wang, C. Chapman, G. C. Schatz, and E. A. Weiss, ACS Nano **11**, 5041 (2017).

[43] H. Ammari and J. C. Nedelec, Methods Verf. Math. Phys. **642**, 174 (1997).

[44] J. J. Rodriguez and A. Salam, J. Phys. Chem. B **115**, 5183 (2011).

[45] C. R. Jacob and M. Reiher, Int. J. Quantum Chem. **112**, 3661 (2012).

SUPPORTING INFORMATION: RESONANCE ENERGY TRANSFER IN ARBITARY MEDIA: BEYOND THE POINT DIPOLE APPROXIMATION

A. Derivation of matrix element beyond dipole approximation

As we explained in the main text, the emitted field can be calculated on the basis of a multipole expansion of the current density by means of the dyadic Green's functions $\overleftrightarrow{G}(\mathbf{R};\omega)$ and $\overleftrightarrow{G}^m(\mathbf{R};\omega)$. By means of the first term of the current density expansion we write quite simple formulas for the electric ($\mathbf{E}^{ED}(\mathbf{r};\omega)$) and magnetic ($\mathbf{B}^{ED}(\mathbf{r};\omega)$) fields from the electric dipole source can be found as [25]:

$$\begin{aligned}\mathbf{E}^{ED}(\mathbf{r};\omega) &= \mu_0\omega^2\overleftrightarrow{G}(\mathbf{r};\omega).\mathbf{p}(\omega)\\ \mathbf{B}^{ED}(\mathbf{r};\omega) &= c^{-1}\mu_0\omega^2\overleftrightarrow{G}^m(\mathbf{r};\omega).\mathbf{p}(\omega),\end{aligned} \tag{S1}$$

The second term of the current density expansion can give us the fields generated by the magnetic dipole current density $\mathbf{m}$:

$$\begin{aligned}\mathbf{B}^{MD}(\mathbf{r};\omega) &= c^{-2}\mu_0\omega^2\overleftrightarrow{G}(\mathbf{r};\omega).\mathbf{m}(\omega)\\ \mathbf{E}^{MD}(\mathbf{r};\omega) &= -c^{-1}\mu_0\omega^2\overleftrightarrow{G}^m(\mathbf{r};\omega).\mathbf{m}(\omega).\end{aligned} \tag{S2}$$

And also the electric field and the magnetic field from an electric quadrupole source:

$$\begin{aligned}\mathbf{E}^{EQ}(\mathbf{r},\omega) &= -\mu_0\omega^2\overleftrightarrow{Q}:\nabla\overleftrightarrow{G}(\mathbf{r},\omega)\\ \mathbf{B}^{EQ}(\mathbf{r},\omega) &= -c^{-1}\mu_0\omega^2\overleftrightarrow{Q}:\nabla\overleftrightarrow{G}^m(\mathbf{r},\omega)\end{aligned} \tag{S3}$$

The matrix element is defined based on the interaction of multiples of the donor with corresponding multipoles of the acceptor [29, 30, 36]

$$\begin{aligned}M^{ee}+M^{mm} &= \left[\mu_i^A\mu_j^D + m_i^A m_j^D/c^2\right]V_{ij}\\ M^{eq}+M^{qe} &= \left[\mu_i^A q_{jk}^D + q_{jk}^A\mu_i^D\right]V_{ijk}\\ M^{qq} &= q_{ik}^A q_{jl}^A V_{ijkl}\\ M^{em}+M^{me} &= Im\left[\mu_i^A m_j^D/c + m_i^A\mu_j^D/c\right]U_{ij}\\ M^{mq}+M^{qm} &= Im\left[m_i^A q_{jk}^D/c + q_{jk}^A m_i^D/c\right]U_{ijk}\end{aligned} \tag{S4}$$

Here c is the velocity of light and $\mu^(A/D)$, $m^(A/D)$ are the electric and magnetic transition moments and and $Q^(A/D)$ is the electric quadrupole transition moment of donor(D)/acceptor(A) respectively. It should be noted that the magnetic transition moment tensor is purely imaginary, i.e. $\mathrm{Im}(m_j) = -im_j$.

Comparing our electric Green function ($\overleftrightarrow{G}$) used in this work with the one in references [29, 30, 40], there are some coefficients that can be derived simply to have the compatible expression for the coupling tensors of V_{ij}, V_{ijk} and V_{ijkl} as follow:

$$\begin{aligned} V_{ij} &= -\mu_0\omega^2 G_{ij}, \\ V_{ijk} &= \mu_0\omega^2 \nabla_k G_{ji}, \\ V_{ijkl} &= \mu_0\omega^2 \nabla_i \nabla_j G_{kl}. \end{aligned} \tag{S5}$$

The coefficients of the coupling tensor for the magnetic Green function ($\overleftrightarrow{G}^m$) are different [29, 36],

$$\begin{aligned} U_{ij} &= -i\mu_0\omega^2 G^m_{ij}, \\ U_{ijk} &= -i\mu_0\omega^2 \nabla_k G^m_{ji}. \end{aligned} \tag{S6}$$

Since we can separate the interaction of electric dipole, magnetic dipole and the electric quadrupole from the donor side with the corresponding multipole of the acceptor, for the ease of convenience we rearrange these interactions into three equations:

$$\mathcal{M}(\mathbf{r}_A, \mathbf{r}_D, \omega) = M^e(\mathbf{r}_A, \mathbf{r}_D, \omega) + M^m(\mathbf{r}_A, \mathbf{r}_D, \omega) + M^q(\mathbf{r}_A, \mathbf{r}_D, \omega), \tag{S7a}$$

(S7b)

$$\begin{aligned} M^e &= M^{ee} + M^{em} + M^{eq} \\ &= \boldsymbol{\mu}^A . \left[\overleftrightarrow{V} . \boldsymbol{\mu}^D - \overleftrightarrow{U} . \frac{i\mathbf{m}^D}{c} . + \overleftrightarrow{Q}^D : \overleftrightarrow{V} \right] \end{aligned} \tag{S7c}$$

(S7d)

$$\begin{aligned} M^m &= M^{me} + M^{mm} + M^{mq} \\ &= -i\frac{m^A}{c} \left[\overleftrightarrow{U} . \boldsymbol{\mu}^D + \overleftrightarrow{V} . \frac{i\mathbf{m}^D}{c} + \overleftrightarrow{U} : \overleftrightarrow{Q}^D \right] \end{aligned} \tag{S7e}$$

(S7f)

$$\begin{aligned} M^q(\mathbf{r}_A, \mathbf{r}_D, \omega) &= M^{qe} + M^{qm} + M^{qq} \\ &= \overleftrightarrow{Q}^A : \left[-\nabla(\overleftrightarrow{V} . \boldsymbol{\mu}^D) + \nabla(\overleftrightarrow{U} . \frac{i\mathbf{m}^D}{c}) + \nabla(\overleftrightarrow{Q}^D : \nabla \overleftrightarrow{V}) \right]. \end{aligned} \tag{S7g}$$

After plugging in the corresponding terms from Eq. S5 and Eq. S6 into Eq. S4 and some algebra we get the main expression in Eq. 22d.

B. Proof of $M^{eq} = -M^{qe}$ and $M^{em} = M^{me}$ for a special case

When the donor and the acceptor have the same identity and orientation, we have the relations:

$$M^{eq} = -M^{qe}, \tag{S8}$$

$$M^{em} = M^{me}. \tag{S9}$$

In the following proof for these relations, we shall see that the reason for the opposite signs in the two equations comes from the fact that the electric Green's function ($\overleftrightarrow{G}$) is a symmetric tensor, while the magnetic Green's function ($\overleftrightarrow{G}^m$) is antisymmetric.

First, let us look at the proof of Eq. S8, starting from the expression of M^{qe}, and recasting it into the matrix element form. Suppose the transition dipole moments for both the donor and the acceptor are $\boldsymbol{\mu}^D = \boldsymbol{\mu}^A = \boldsymbol{\mu}$, and the quadrupole moment is $\overleftrightarrow{Q}^D = \overleftrightarrow{Q}^A = \overleftrightarrow{Q}$. Then, the coupling term M^{qe} is the interaction between $\overleftrightarrow{Q}^A$ and the gradient of the electric field from $\boldsymbol{\mu}^D$:

$$\begin{aligned}
M^{qe} &= -\overleftrightarrow{Q}^A : \nabla \mathbf{E}^{D,\boldsymbol{\mu}} = -\overleftrightarrow{Q}^A : \left[\nabla\left(\mu_0\omega^2 \overleftrightarrow{G}\cdot\boldsymbol{\mu}^D\right)\right] \\
&= -\mu_0\omega^2 \sum_{jk} Q_{jk}\left[\nabla\left(\overleftrightarrow{G}\cdot\boldsymbol{\mu}\right)\right]_{jk} = -\mu_0\omega^2 \sum_{jk} Q_{jk}\left[\nabla_k\left(\overleftrightarrow{G}\cdot\boldsymbol{\mu}\right)_j\right] \\
&= -\mu_0\omega^2 \sum_{jk} Q_{jk}\left[\nabla_k\left(\sum_l G_{jl}\mu_l\right)\right] = -\mu_0\omega^2 \sum_{jk} Q_{jk}\left[\nabla_k\left(\sum_l \mu_l G_{lj}\right)\right] \\
&= -\mu_0\omega^2 \sum_{jkl} Q_{jk}\nabla_k\mu_l G_{lj} = -\mu_0\omega^2 \sum_{jkl} Q_{jk}\nabla_k\mu_l G_{jl}.
\end{aligned} \tag{S10}$$

Note that we utilize the symmetric property of the $\overleftrightarrow{G}$ tensor in the last step, i.e. $G_{lj} = G_{jl}$. On the other hand, the coupling term M^{eq} is the interaction between $\boldsymbol{\mu}^A$ and the electric field from $\overleftrightarrow{Q}^D$:

$$\begin{aligned}
M^{eq} &= -\boldsymbol{\mu}^A \cdot \mathbf{E}^{D,\overleftrightarrow{Q}} = -\boldsymbol{\mu}^A \cdot \left[-\mu_0\omega^2\left(\overleftrightarrow{Q}^D : \nabla\overleftrightarrow{G}\right)\right] \\
&= \mu_0\omega^2 \sum_l \mu_l \left(\overleftrightarrow{Q}^D : \nabla\overleftrightarrow{G}\right)_l = \mu_0\omega^2 \sum_l \mu_l \left(\sum_{jk} Q_{jk}\nabla_k G_{jl}\right) \\
&= \mu_0\omega^2 \sum_{jkl} \mu_l Q_{jk}\nabla_k G_{jl} = \mu_0\omega^2 \sum_{jkl} Q_{jk}\nabla_k\mu_l G_{jl} \\
&= -M^{qe}.
\end{aligned} \tag{S11}$$

The final equation is made possible by the fact that the donor and the acceptor have the same electric dipole and quadrupole, as specified earlier.

Following a similar path, we can prove the second relation, Eq. S9. Suppose that the magnetic dipoles are $\mathbf{m}^D = \mathbf{m}^A = \mathbf{m}$, and the electric dipoles are $\boldsymbol{\mu}^D = \boldsymbol{\mu}^A = \boldsymbol{\mu}$. Starting from the M^{em} term, we have:

$$\begin{aligned}
M^{em} &= -\boldsymbol{\mu}^A \cdot \mathbf{E}^{D,\mathbf{m}} = -\boldsymbol{\mu}^A \cdot \left[-c^{-1}\mu_0\omega^2 \left(\overleftrightarrow{G}^M \cdot \mathbf{m}^D\right)\right] \\
&= c^{-1}\mu_0\omega^2 \sum_j \mu_j \left(\overleftrightarrow{G}^M \cdot \mathbf{m}\right)_j = c^{-1}\mu_0\omega^2 \sum_j \mu_j \left(\sum_k G^M_{jk} m_k\right) \\
&= c^{-1}\mu_0\omega^2 \sum_j \mu_j \left(\sum_k m_k G^M_{kj}\right) = c^{-1}\mu_0\omega^2 \sum_j \mu_j \left(\sum_k m_k (-G^M_{jk})\right) \\
&= -c^{-1}\mu_0\omega^2 \sum_{jk} \mu_j m_k G^M_{jk} = -c^{-1}\mu_0\omega^2 \sum_{jk} m_k G^M_{kj} \mu_j \\
&= -c^{-1}\mu_0\omega^2 \sum_k m_k \left(\sum_j G^M_{kj}\mu_j\right) = -c^{-1}\mu_0\omega^2 \sum_k m_k \left(\overleftrightarrow{G}^M \cdot \boldsymbol{\mu}\right)_k \\
&= -c^{-1}\mu_0\omega^2 \mathbf{m} \cdot \left(\overleftrightarrow{G}^M \cdot \boldsymbol{\mu}\right) = -\mathbf{m}^A \cdot \left[c^{-1}\mu_0\omega^2 \left(\overleftrightarrow{G}^M \cdot \boldsymbol{\mu}^D\right)\right] \\
&= -\mathbf{m}^A \cdot \mathbf{B}^{D,\boldsymbol{\mu}} = M^{me}.
\end{aligned} \tag{S12}$$

C. Green function for dispersive, absorptive, infinitely homogeneous, nonconductive medium

According to Drude-Born-Fedorov equations [43], field operators in a dielectric medium that is dispersive, absorptive, infinitely homogeneous, nonconductive, with no free charges, and chiral can be defined as

$$\begin{aligned}
\overleftrightarrow{G}_{hom}(\mathbf{R};\omega) &= \frac{\gamma}{4\pi}\left[\frac{1}{\gamma R}\left(\mathbf{U} - \hat{\mathbf{R}}\hat{\mathbf{R}}\right) - \left[\frac{1}{(\gamma R)^2} - \frac{1}{(\gamma R)^3}\right]\left(\mathbf{U} - 3\hat{\mathbf{R}}\hat{\mathbf{R}}\right)\right] e^{\gamma.\mathbf{R}}, \\
\overleftrightarrow{G}^M_{hom}(\mathbf{R};\omega) &= \frac{\gamma}{4\pi}\left[\frac{1}{\gamma R} - \frac{1}{(\gamma R)^2}\right] e^{\gamma.\mathbf{R}} \mathbf{U} \times \hat{\mathbf{R}},
\end{aligned} \tag{S13}$$

and γ, the magnitude of wavevector is given by

$$\gamma^{(\pm)}(\omega) = \frac{k(\omega)}{1 \mp k(\omega)\beta(\omega)} = \gamma'^{(\pm)}(\omega) + i\gamma''^{(\pm)}(\omega). \tag{S14}$$

We should note that $+$ and $-$ denote left-circularly polarized and right-circularly polarized field components, respectively. If we define $\gamma''^{(\pm)}(\omega)$ be strictly positive, the wave is absorbed by the medium and is not amplified by it.

The complex chirality admittance of the medium is defined by β in Eq. (S14) and the properties of the chiral medium are included within these electromagnetic field operators. If $\beta(\omega) > 0$, the chiral medium is left-handed, while $\beta(\omega) < 0$ corresponds to a right-handed medium.

Chiral media refers to a general class of bianisotropic media, responding with both electric and magnetic polarization to excitation by electric and magnetic fields. The chiral media couplings to these fields are described by a generalized set of fundamental relations. The strength of coupling is determined by the magnitude of chirality admittance, β which assesses the bulk magneto-electric properties of the material[44].

D. Calculating transition electric dipole, magnetic dipole, and electric quadrupole matrix elements: quantum electrodynamics approach

Employing time-dependent perturbation theory, we investigate the interaction of a particle with classical (i.e., non-quantized) electromagnetic radiation. The Hamiltonian of such a system is expressed as

$$H = \frac{1}{2m}\left(\mathbf{p} - \frac{e}{c}\mathbf{A}\right)^2 + V_s = H_0 + H_{int} \tag{S15}$$

where H_0 is the Hamiltonian in the absence of the field and H_{int} is the matter-field interaction Hamiltonian. Adopting the Coulomb gauge, $\nabla \cdot \mathbf{A} = 0$ and supposing that the perturbation corresponds to a monochromatic plane-wave of angular frequency ω, H_{int} becomes

$$H_{int} \simeq -\frac{e}{mc}\mathbf{A}.\mathbf{p} = -\frac{e}{mc}A_0\cos(\mathbf{k}.\mathbf{R} - \omega t)\hat{\mathbf{e}}.\mathbf{p} \tag{S16}$$

$$= \frac{e}{mc}A_0\left(e^{i(\mathbf{k}.\mathbf{R}-\omega t)} + e^{-i(\mathbf{k}.\mathbf{R}-\omega t)}\right)\hat{\mathbf{e}}.\mathbf{p} \tag{S17}$$

$$= M(\mathbf{k})e^{-i\omega t} + M(\text{-}\mathbf{k})e^{i\omega t} \tag{S18}$$

Correspondingly, the first(second) term on the right-hand side of Eq. (S18) describes a process by which the atom absorbs(emits) energy $\hbar\omega$ from the electromagnetic field.In other word this can be decoded as the absorption and stimulated emission of a photon of energy $\hbar\omega$ by the particle respectively.

Using the Fermi's Golden rule to calculate the rate of transition induced by H_{int}, we see

$$W_{D\longrightarrow A} = \frac{2\pi}{\hbar}|M(\mathbf{r}_A, \mathbf{r}_D, \omega)|^2\rho(\omega) \tag{S19}$$

where ω is the angular frequency of the transferred energy (essentially the excitation energy of the acceptor), $\mathbf{r}_D$ ($\mathbf{r}_A$) is the spatial position of the donor (acceptor) particle, and $\rho(\omega)$ is the density of final states associated with energy ω (corresponding to the excited state of the acceptor and the ground state of the donor).

For a particle of size 10 to 100 Angstroms and the long-wavelength approximation, $e^{-i(\mathbf{k}.\mathbf{R})} \cong 1$, which is known as dipole approximation, the transition rate involves the electric dipole matrix element and as long as this is nonzero, it is called an electric-dipole allowed transition. The magnitude of the transition dipole of the donor (acceptor) from the excited state (the superscript e) of the donor molecule to its ground state (the superscript g) is

$$\mathbf{p}^{ge}(\mathbf{r}_D) = \mu^{ge}(\mathbf{r}_D)\mathbf{e}_D = \int d\tau \Psi_g^*(\mathbf{r}_D)\mathbf{R}\Psi_e(\mathbf{r}_D) \tag{S20}$$

$$\mathbf{p}^{eg}(\mathbf{r}_A) = \mu^{eg}(\mathbf{r}_A)\mathbf{e}_A = \int d\tau \Psi_e^*(\mathbf{r}_A)\mathbf{R}\Psi_g(\mathbf{r}_A) \tag{S21}$$

Keeping the second term in the expansion of $e^{-i(\mathbf{k}.\mathbf{R})}$, the corresponding terms for the magnetic dipole and electric quadrupole matrix elements are:

$$\begin{aligned} \mathbf{m}^{km}(\mathbf{r}) &= \frac{e}{2mc} < k|\mathbf{L}|m >= \frac{e}{2mc}\int d\tau \Psi_k^*(\mathbf{r}_D)\mathbf{L}\Psi_m(\mathbf{r}_D) \\ (\mathbf{q}^{km})_{ij} &=< k|(er_i)(er_j)|m > \end{aligned} \tag{S22}$$

where $\mathbf{L}$ is the orbital angular momentum $\mathbf{L} = \mathbf{r} \times \mathbf{p}$.

If we take into account the interaction of the magnetic component of the electromagnetic wave with the electron's spin and orbital magnetic moment, the complete quantity that mediates magnetic dipole transitions between different atomic states is defined as

$$\mathbf{m}^{total} = \frac{e}{2mc} < k|\mathbf{L} + 2\mathbf{S}|m > \tag{S23}$$

where $\mathbf{S}$ is the electron spin operator. However, for the magnetic transition moments, the spin contributions can be ignored since for states with a multiplicity larger than zero (i.e., for $S > 0$) the different M_S-components of the multiplet will be degenerate [45] and the components with $+M_S$ and $-M_S$ provide spin contributions to the magnetic transition moments that cancel each other.

E. Additional figures

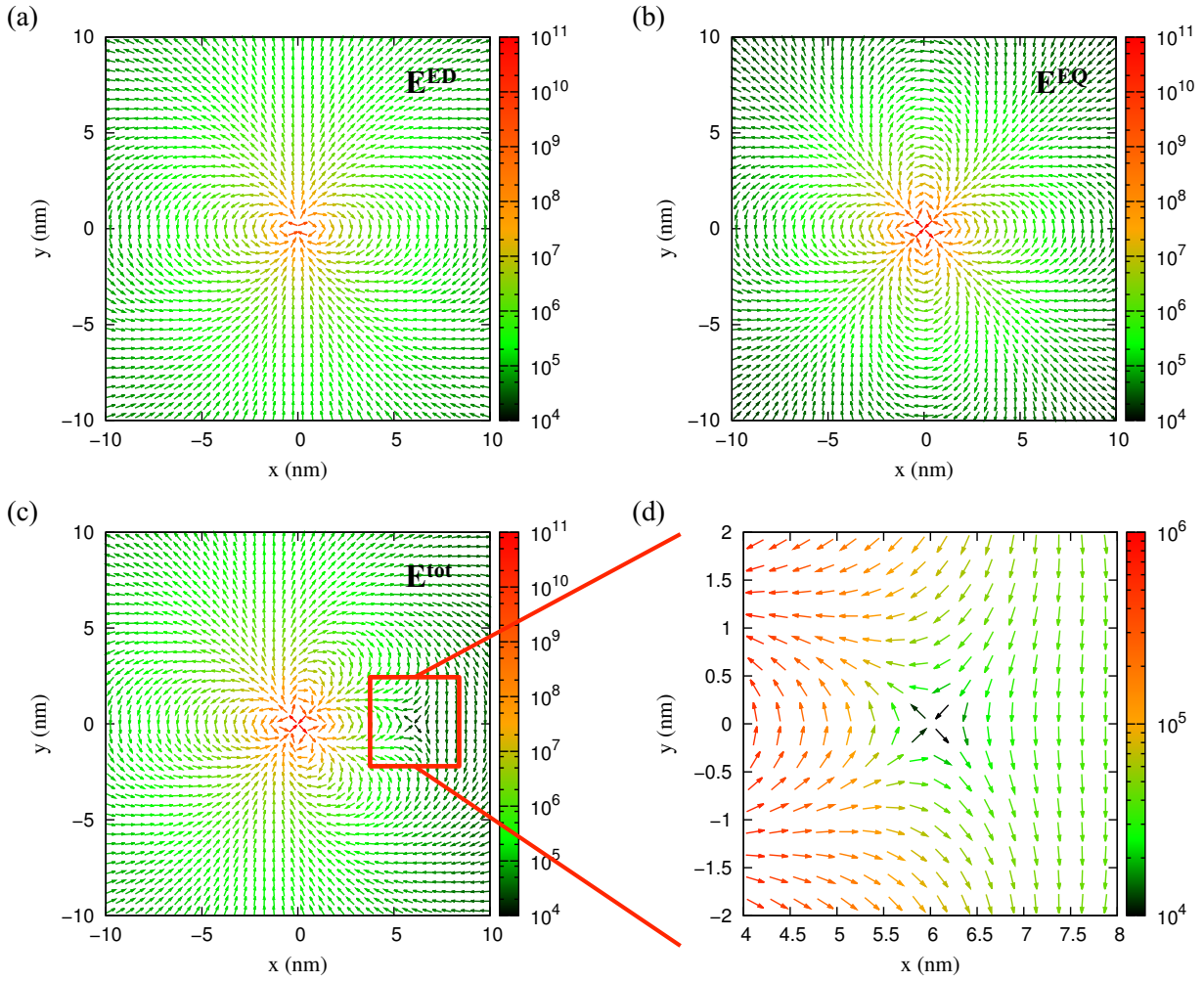

FIG. S1. The vector maps, for Case 1, of the electric fields of dipole ($\mathbf{E}^{ED}$) (a) and quadrupole ($\mathbf{E}^{EQ}$) (b), and the total field of both dipole and quadrupole ($\mathbf{E}^{tot}$) (c). The spatial plane is the xy plane with $z = 0$ nm. The vectors only represent the real part of x and y components of the electric fields.

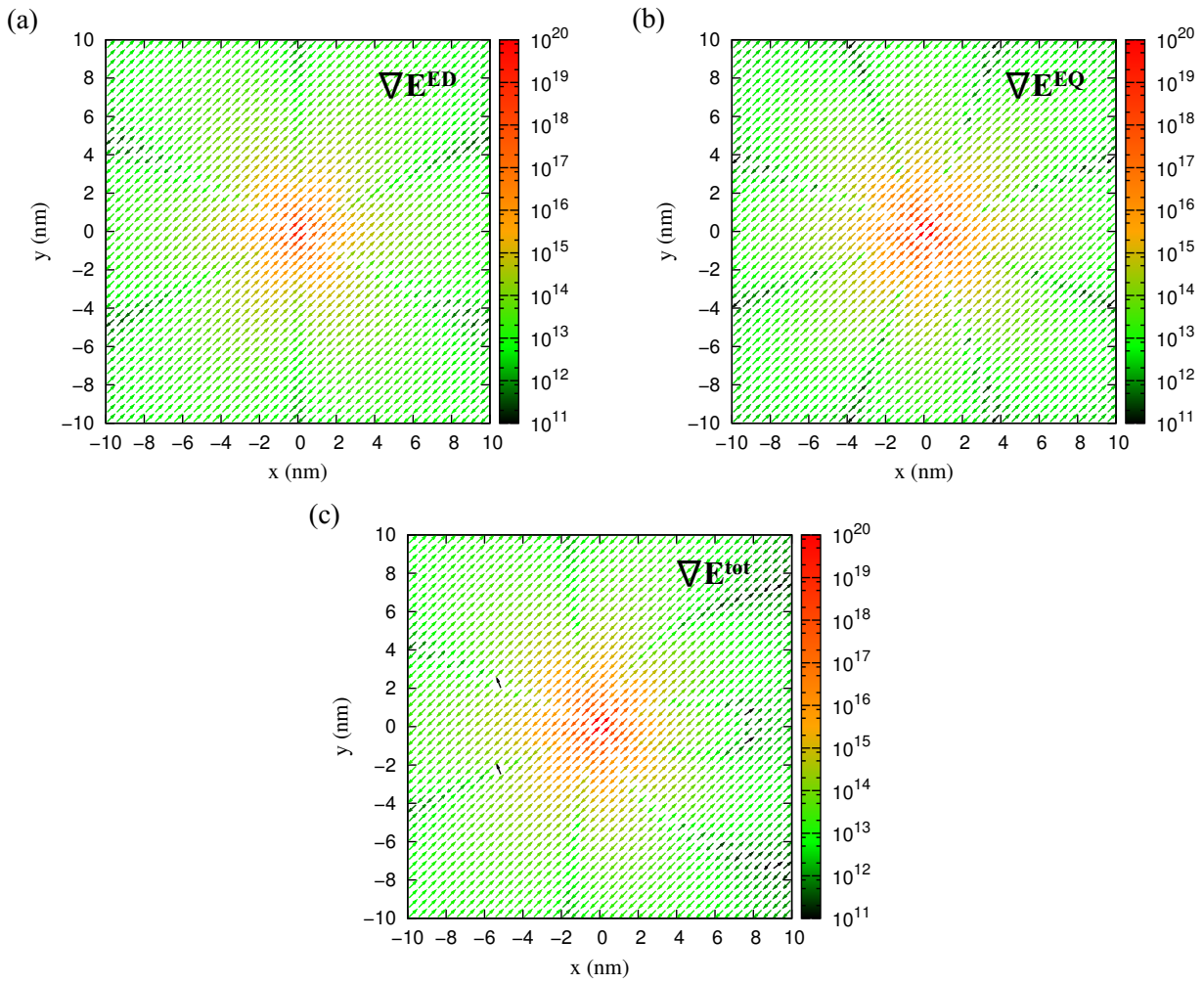

FIG. S2. The vector maps, for Case 1, of the electric field gradients of dipole ($\nabla \mathbf{E}^{ED}$) (a) and quadrupole ($\nabla \mathbf{E}^{EQ}$) (b), and the gradient of the total field ($\nabla \mathbf{E}^{tot}$) (c). The spatial plane is the xy plane with $z = 0$ nm. The vectors only represent the real part of xy and yx components of the electric fields.

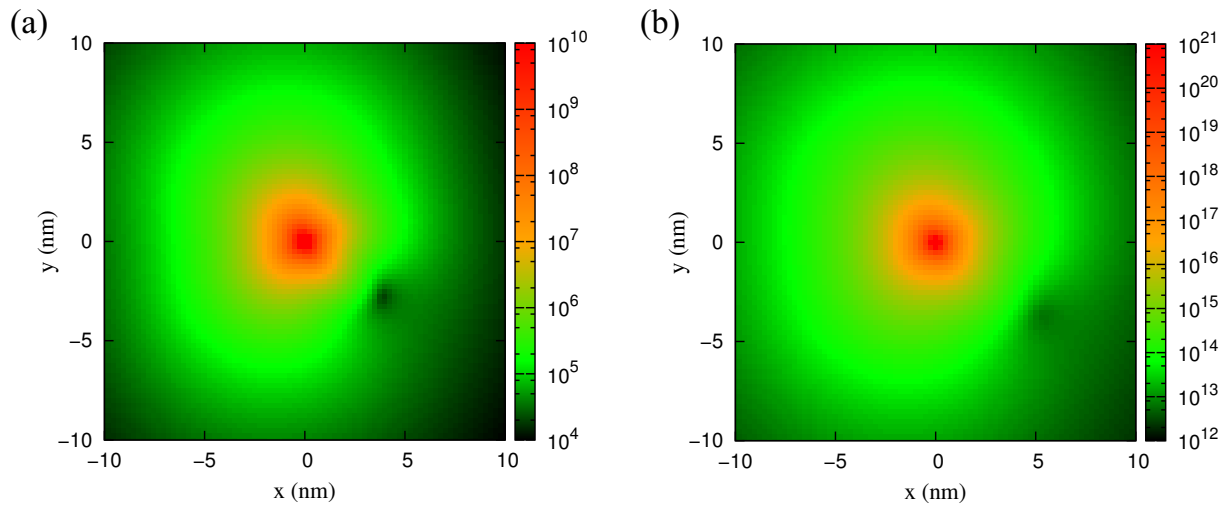

FIG. S3. The heat maps, for Case 2, of the magnitude of the total electric field ($\mathbf{E}^{tot}$) (a) and the magnitude of the gradient of the total electric field ($\nabla\mathbf{E}^{tot}$) (b) in the xy plane whith $z = 0$ nm.

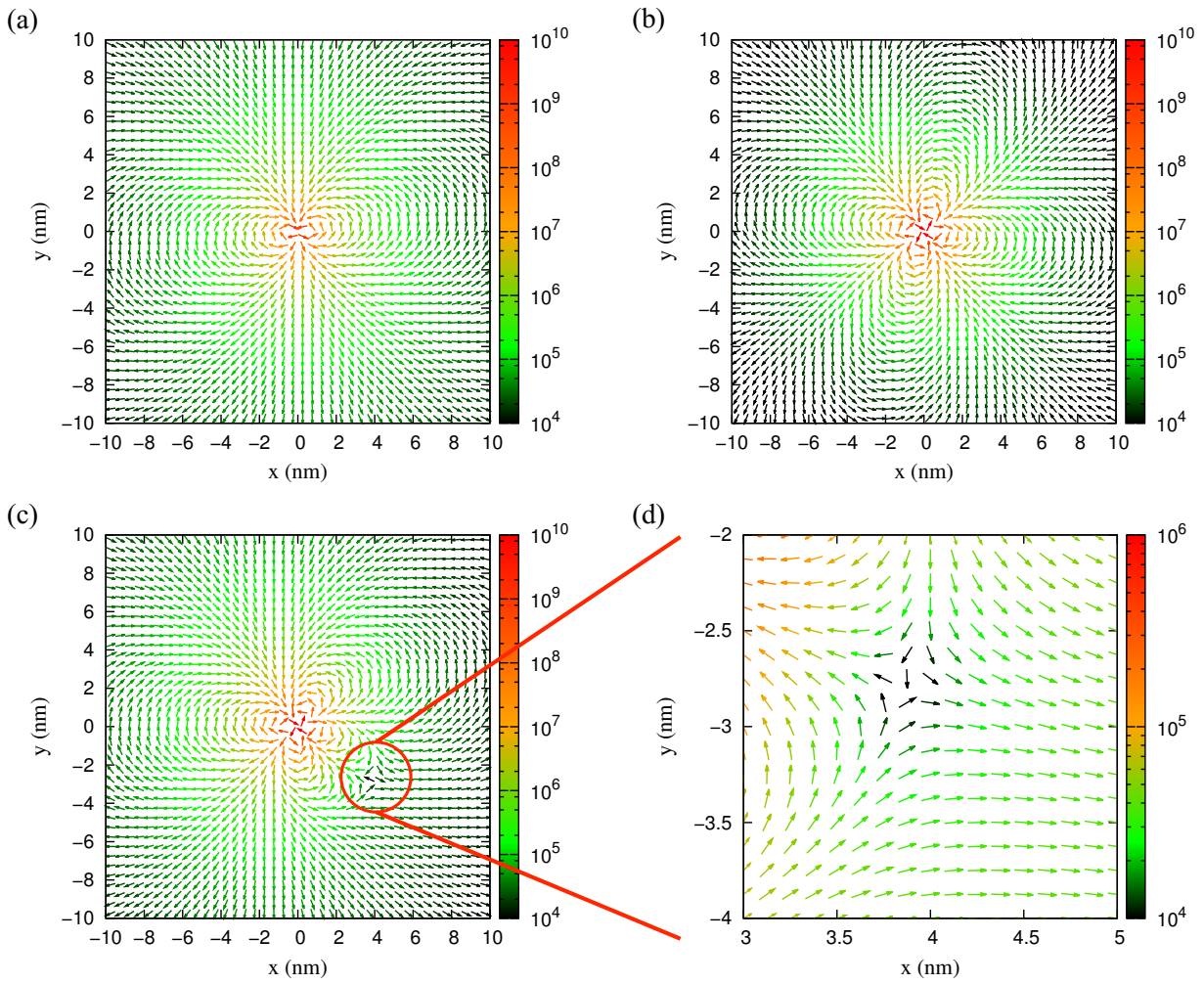

FIG. S4. The vector maps, for Case 2, of the electric fields of dipole ($\mathbf{E}^{ED}$) (a) and quadrupole ($\mathbf{E}^{EQ}$) (b), and the total field of both dipole and quadrupole ($\mathbf{E}^{tot}$) (c). The spatial plane is the xy plane with $z = 0$ nm. The vectors only represent the real part of x and y components of the electric fields.